

γ -Ray irradiation of liposomes of polymerizable phospholipids containing octadeca-2,4-dienoyl groups and characterization of the irradiated liposomes

Kazuhiro Akama,^{*†‡} Yoshihiro Yano,^a Satoru Tokuyama,^{†‡} Fumio Hosoi^{b§} and Hideki Omichi^{b¶}

^aTsukuba Research Laboratory, NOF Corporation, 5-10 Tokodai, Tsukuba, Ibaraki, 300-2635, Japan

^bTakasaki Radiation Chemistry Research Establishment, Japan Atomic Energy Research Institute, 1233, Watanuki-machi, Takasaki, Gunma, 370-1207, Japan

Received 29th October 1999, Accepted 18th January 2000

The synthesis of a variety of polymerizable phospholipids containing the octadeca-2,4-dienoyl moiety on 2-acyl chains and the characteristics of liposomes containing those phospholipids of the γ -irradiation are described. We synthesized three different polymerizable phosphocholines that have different 1-acyl chain lengths with the octadeca-2,4-dienoyl moiety on the 2-acyl chain: myristoyl (MODPC), palmitoyl (PODPC) and stearoyl (SODPC). The liposomes were prepared by extrusion through polycarbonate filters with a pore size of 0.2 μm , and were polymerized by γ -irradiation with various dose rates. The polymerization rate increased in the order SODPC > MODPC > PODPC. The mechanism of the polymerization of SODPC was the same as that of 1,2-bis-[(*E,E*)-octadeca-2,4-dienoyl]-*sn*-glycero-3-phosphocholine (DODPC), but differed from that of MODPC and PODPC. Freeze–thaw testing was used to evaluate the stability of the polymerizable liposomes. The MODPC liposome was more stable than other monofunctional liposomes. For similar irradiation, the polymerization behavior of the liposomes was significantly affected by the 1-acyl length.

Introduction

Liposomes are well known as biomimetic membranes that self-organize when phosphocholine is dispersed in water. Liposomes can encapsulate drugs, such as anticancer agents, proteins, and other bioactive materials. Much attention has been paid to applications of carriers for drug delivery systems. However, conventional, unmodified liposomes without additives (*e.g.* DPPC) have low stability against physical and chemical stimuli, resulting in changes of diameter and leakage of inner substances caused by fusion and fission *in vitro*¹ and *in vivo*.^{2,3} Liposomes can be stabilized by the polymerization of phospholipids contained in the membrane.⁴ Diacetylenic,^{5,6} butadienic,^{5,7–9} vinylic,¹⁰ methacryloylic^{7,11} and thiolic^{12,13} units have been used as polymerizable units in acyl chains. Since Akimoto *et al.* synthesized 1,2-bis[(*E,E*)-octadeca-2,4-dienoyl]-*sn*-glycero-3-phosphocholine (DODPC), which contains two butadienic moieties in the acyl chains attached to phosphocholine,⁹ researchers have studied various methods for the polymerization of liposomes, by UV irradiation,¹⁴ organic initiators,^{15,16} redox initiators,¹⁷ and γ -irradiation.^{14,17} Ohno *et al.* reported selective polymerization of 1- or 2-acyl chains of DODPC by using appropriate radical initiators.^{15,16} In particular, γ -ray polymerization is one of the best methods for encapsulating a drug in liposomes, because it requires no residual initiators, produces less degradation and denaturing of

encapsulated substances, and polymerizes the liposomes at temperature as low as 4 °C. The γ -ray polymerization of DODPC liposomes yielded high polymerization conversion (70–80%) and the liposomes were stable against physical stimuli, such as repeated freeze–thawing.¹⁸

We developed previously a liposome type of artificial red blood cell (called artificial red cells, or ARC), which encapsulates hemoglobin with DODPC. For the γ -ray polymerization of the membrane of ARC, we observed no change in diameter and no leakage of hemoglobin, even after repeated freeze–thaw cycles.¹⁹ The polymerized ARC was stable in the blood stream without aggregating, and showed no toxicity or side effects.¹⁸ In contrast to the attention given to the stability of the liposomes, little attention has been given to the mechanism of polymerization using γ -irradiation.¹⁷ Recently, we reported the polymerization of DODPC liposomes using γ -irradiation and found that polymerization of DODPC liposomes by γ -rays gave selective polymerization between the 1- and 2-acyl chains.²⁰

We report here (a) the synthesis of polymerizable phospholipids that have different 1-acyl chain lengths with the same polymerizable moieties on 2-acyl chains of phosphocholine, (b) characteristics of polymerization by γ -radiation compared with those of DODPC liposomes, and (c) the stability of polymerized liposomes against freeze–thawing.

Results

Synthesis of polymerizable phospholipids

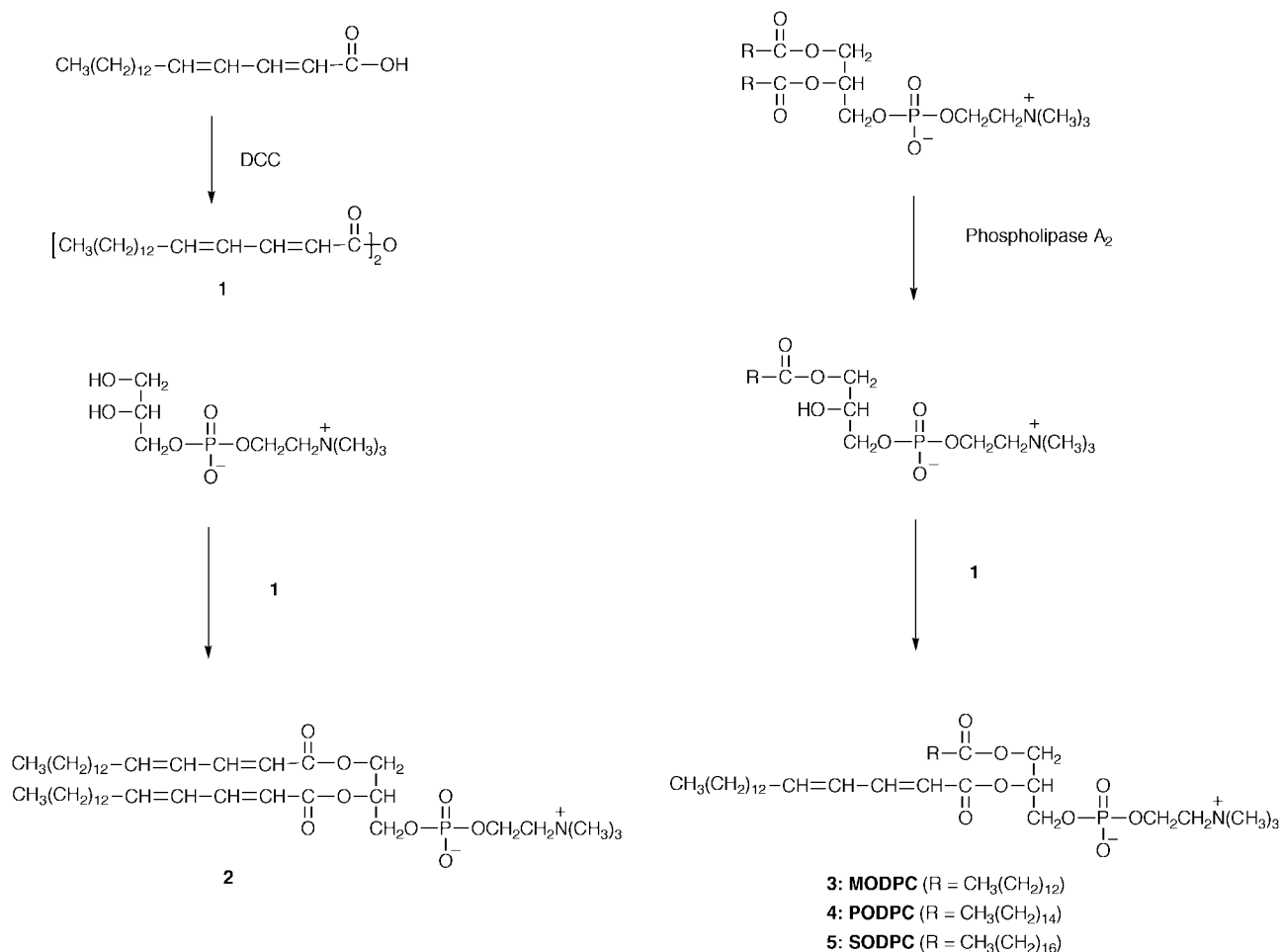
Scheme 1 shows the method for synthesizing the chemical structures of the polymerizable phospholipids (2–5). We synthesized DODPC 2, which has two polymerizable groups in the 1- and 2-acyl chains, from *L*- α -glycerophosphorylcholine (GPC) and (*E,E*)-octadeca-2,4-dienoyl anhydride 1. We also synthesized MODPC 3, PODPC 4, and SODPC 5 from

[†]Present address: Medical Materials Business Dept., Oleo & Speciality Chemicals Division, NOF Corporation, 4-20-3 Ebisu, Shibuya-ku, Tokyo 150-6019, Japan. Tel +81-3-5424-6692; Fax +81-3-5424-6810; E-mail: kazuhiro_akama@nof.co.jp

[‡]Present address: Oleochemicals Research Laboratory, NOF Corporation, 1-56 Ohama-cho, Amagasaki, Hyogo 660-0095, Japan.

[§]Deceased March 13, 1998.

[¶]Present address: Japan Atomic Energy Research Institute Washington Office, 1825 K Street, N.W., Suite 508, Washington, DC 20006-1202, USA.



Scheme 1 Synthetic scheme for preparation of the polymerizable phospholipids.

hydrolyzed diacyl phosphatidylcholine, corresponding to 1-acyl lysophosphorylcholine and (*E,E*)-octadeca-2,4-dienoyl anhydride. The phospholipids were purified twice using chromatography on silica gel and freeze-dried. They were isolated as white colorless powders without polymers.

Surface pressure–area isotherms

Fig. 1 shows the surface pressure–area isotherms for various polymerizable phospholipids. The monolayers of SODPC were

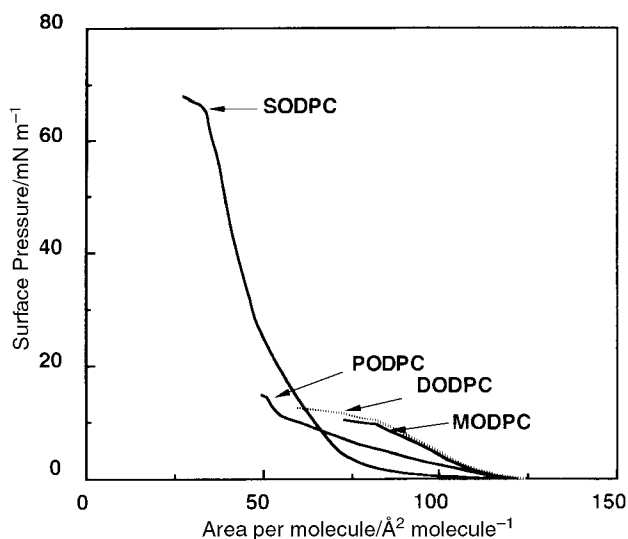


Fig. 1 Surface pressure–area isotherms of various polymerizable phospholipids measured at 3.8 °C.

easily compressed under these conditions, *i.e.* a temperature of 4 °C. The monolayers of DODPC and other monofunctional phospholipids, MODPC and PODPC, collapsed before reaching a less compressible region. For monofunctional polymerizable phospholipids, the order of compressibility was SODPC > PODPC > MODPC.

Preparation of liposomes

The liposomes were prepared by an extrusion method. The phase-transition temperatures (T_c) of the polymerizable liposomes of MODPC, PODPC and SODPC were determined by DSC (see Table 1). The T_c for MODPC, PODPC, and SODPC liposomes, which contain saturated fatty acyl chains in the 1-acyl moiety, were lower than those of the saturated diacylphosphatidylcholines (*e.g.*, the T_c values for 1,2-dimyristoyl-*sn*-glycero-3-phosphocholine (DMPC), 1,2-dipalmitoyl-*sn*-glycero-3-phosphocholine (DPPC), and 1,2-distearoyl-*sn*-glycero-3-phosphocholine (DSPC) are 23, 41, and 58 °C, respectively²¹), which corresponds to the length of the fatty 1-acyl chain in the polymerizable phospholipids. The measured T_c increased with increasing length of the methylene units of 1-acyl chains. The values of λ_{max} and the molecular absorption coefficient (ϵ_{max}) corresponding to maximum absorption for MODPC, PODPC, and SODPC liposomes are also given in Table 1. Above T_c , $\lambda_{\text{max}} = 259$ nm, and below T_c , $\lambda_{\text{max}} = 253$ nm. The values of λ_{max} obtained for PODPC liposomes were identical with those reported by Takeoka *et al.*²² For SODPC liposomes which contain two more methylene units than PODPC, and for MODPC which contains two methylene units fewer than PODPC, our measured values of λ_{max} were the same as those for the PODPC liposomes. The

Table 1 Phase-transition temperatures (T_c), λ_{\max} and ϵ_{\max} of polymerizable phospholipids containing octadeca-2,4-dienoyl groups as liposomes

Compound	$T_c/^\circ\text{C}$	λ_{\max}/nm		$\epsilon_{\max} \times 10^4/\text{L mol}^{-1} \text{cm}^{-1}$	
		Below T_c	Above T_c	Below T_c	Above T_c
MODPC ^b	16.6	253.5	259.9	2.22	2.44
PODPC ^c	28.2	253.5	259.5	2.17	2.36
	28.0 ^a	253.0 ^a	259.3 ^a	—	—
SODPC ^d	34.0	253.3	259.1	2.10	2.28
DODPC ^e	18.9 ^a	—	256.0	—	4.60

^aFrom ref. 21. ^bThe diameter was 197.0 ± 30.7 nm, SD=15.6%. ^cThe diameter was 164.0 ± 44.7 nm, SD=27.2%. ^dThe diameter was 177.4 ± 51.1 nm, SD=28.8%. ^eThe diameter was 203.2 ± 59.4 nm, SD=28.8%.

value of ϵ_{\max} for each monofunctional polymerizable phospholipid below T_c was about 10% less than that above T_c .

Polymerization of liposomes

Fig. 2 shows the UV spectra of irradiated and monomeric DODPC and MODPC liposome solutions. The λ_{\max} of absorbance of monomeric DODPC and MODPC liposomes was at 256 nm and 259 nm, respectively. The λ_{\max} of both DODPC and MODPC liposomes decreased with increasing irradiation time. To ensure 100% yield of polymerization conversion, we directly irradiated the quartz cell containing the diluted monomeric liposome solution. The absorption completely disappeared on irradiation with a UV lamp at a wavelength of 254 nm. This baseline agreed with 100% yield of UV-irradiated liposomes (1 wt%) from other experiments, which also did not indicate any residual monomers. The width of the absorption curves of MODPC liposomes decreased to those of the DODPC liposomes.

Fig. 3 shows changes in the polymerization conversion when DODPC liposomes were γ -irradiated at various dose rates. The polymerization conversion increased with increasing irradiation time and increasing dose rate. Furthermore, the polymerization conversions rapidly increased up to 50% and then increased more slowly with additional irradiation. However, under these irradiation conditions the polymerization did not proceed beyond about 90% conversion (dose rate was 3.3 kGy h^{-1} , total irradiation time 16 h).

Fig. 4 shows changes in the polymerization conversion of MODPC, PODPC, and SODPC liposomes. For all liposomes, polymerization conversion increased with increasing irradiation

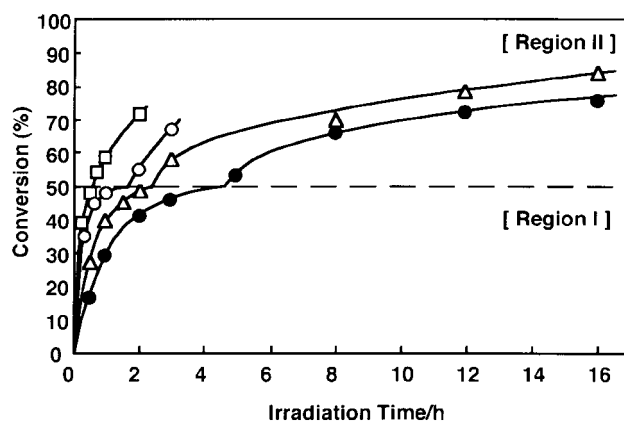


Fig. 3 Effect of dose rate on polymerization conversion of DODPC liposomes. Dose rate: (●); 1.65 kGy h^{-1} , (△); 3.3 kGy h^{-1} , (○); 5.0 kGy h^{-1} and (□); 10.0 kGy h^{-1} .

time, similar to the DODPC liposomes. For similar dose levels, the order of increasing polymerization conversion of liposomes was SODPC > MODPC > PODPC.

DODPC liposomes were hydrolyzed so that DODPC liposome polymers, after irradiation by γ -rays, were insoluble in any organic solvent. To extract the soluble polymer from DODPC polymers, methanolysis of DODPC polymers has been used.¹⁷ However, the methanolysis of DODPC requires relatively high temperatures of 100°C and long reaction times of 2 days. Therefore, we developed a simpler method. Under hydrolysis conditions of 70°C and 24 h, we observed a visual change of the homogeneous liposome solution to a turbid solution after hydrolysis. Then, we confirmed the complete hydrolysis of the DODPC polymers by using IR spectroscopy. The measured molecular weights were reproducible for this protocol. Under these conditions the molecular weight of the polymers might not have an impact on the effectiveness of the hydrolysis. Therefore, the obtained poly(octadeca-2,4-dienoic acid)s were determined by using gel permeation chromatography (GPC). Fig. 5 shows a chromatogram of hydrolyzed poly(octadeca-2,4-dienoic acid)s and octadeca-2,4-dienoic acid. The degrees of polymerization were estimated to be between 15 and 20, corresponding to a molecular weight for octadeca-2,4-dienoic acid of 557, using polystyrene standards. Fig. 6 shows molecular weights of octadeca-2,4-dienoyl polymers that were obtained by hydrolysis of DODPC liposomes. The molecular weight of octadeca-2,4-dienoyl polymers obtained from DODPC liposomes decreased rapidly to an asymptotic limit with irradiation up to 1 h.

Fig. 7 shows the molecular weights of octadeca-2,4-dienoyl polymers obtained by hydrolysis of SODPC liposomes irradiated under various conditions. The molecular weights of the octadeca-2,4-dienoyl polymers obtained from SODPC liposomes were less than those of the DODPC liposomes. The decrease in molecular weight with irradiation was the same as that observed for the DODPC liposomes. The degrees of polymerization of SODPC liposomes were estimated to be

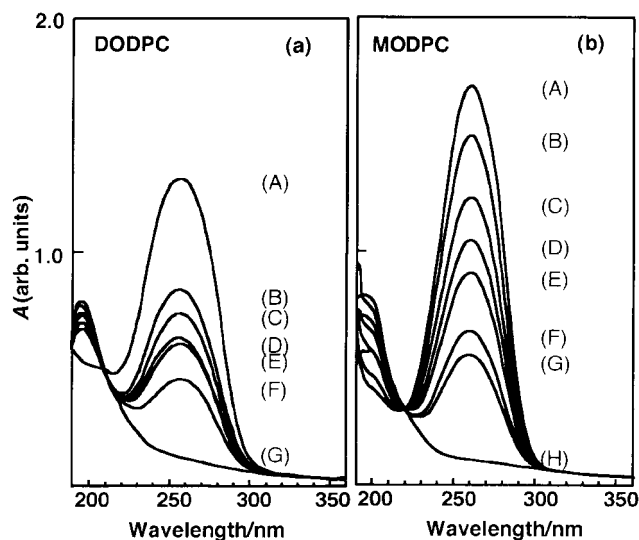


Fig. 2 Change of UV spectra for liposomes during γ -irradiation at 4°C . (a) DODPC liposome, dose rate 10 kGy h^{-1} , (A) before γ -irradiation, (B) 15 min, (C) 30 min, (D) 45 min, (E) 60 min, (F) 120 min, and (G) after UV irradiation. (b) MODPC liposome, dose rate 5 kGy h^{-1} , (A) before γ -irradiation, (B) 0.5 h, (C) 1 h, (D) 1.5 h, (E) 2 h, (F) 3 h, (G) 5 h, and (H) after UV irradiation.

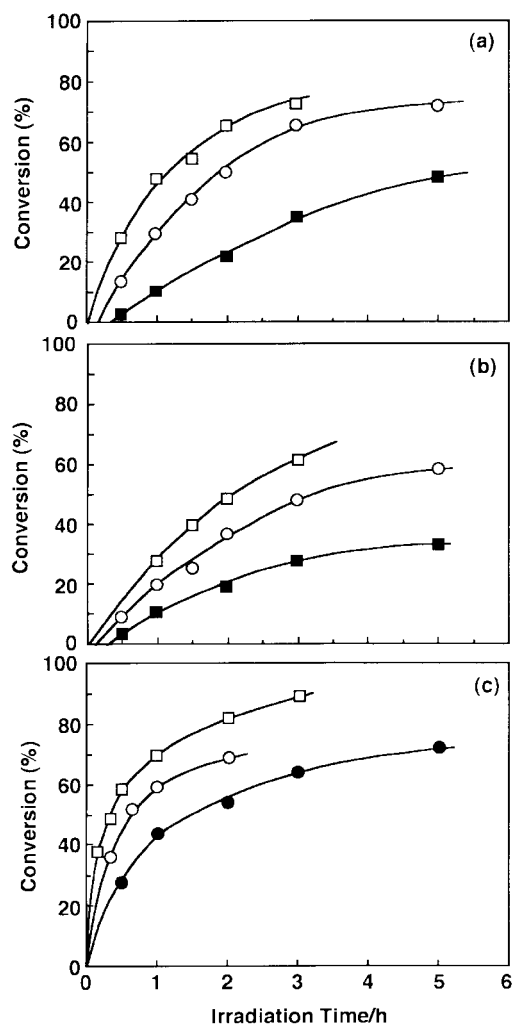


Fig. 4 Effect of dose rate on polymerization conversion of various liposomes. (a) MODPC liposome, (b) PODPC liposome, (c) SODPC liposome. Dose rate: (■); 1.5 kGy h⁻¹, (●); 1.65 kGy h⁻¹, (○); 5.0 kGy h⁻¹, and (□); 10.0 kGy h⁻¹.

between 10 and 14, as described above. On the other hand, the hydrolyzed PODPC and MODPC liposomes were insoluble not only in THF but also in all other polar solvents, such as DMF and DMSO. However, it was observed that the IR spectra of hydrolyzed MODPC and PODPC polymers were identical to those for the SODPC polymers (data not shown). The IR spectra of polymers obtained from the SODPC liposomes were also similar to those of the DODPC liposomes.

Stability of polymerized liposomes

We evaluated the physical stability of the polymerizable liposomes by using freeze-thaw tests. Freeze-thawing is commonly used for trapping drugs in liposomes. However, liposomes composed of a phosphatidylcholine can not retain their structure following freeze-thawing cycles, because either the liposome structure or the diameter of the liposomes is affected by the freezing and thawing.²³ Thus, we used freeze-thawing tests as one evaluation for the stability of liposome membranes.

Fig. 8 shows the changes of mean diameter of polymerized liposomes after one freeze-thaw cycle. The error bar for each point indicates the standard deviation of the mean diameter. Within statistical uncertainty, the diameter of DODPC liposomes did not change after freezing and thawing. On the other hand, a small change was observed in the diameter of monofunctional polymerized liposomes except for MODPC

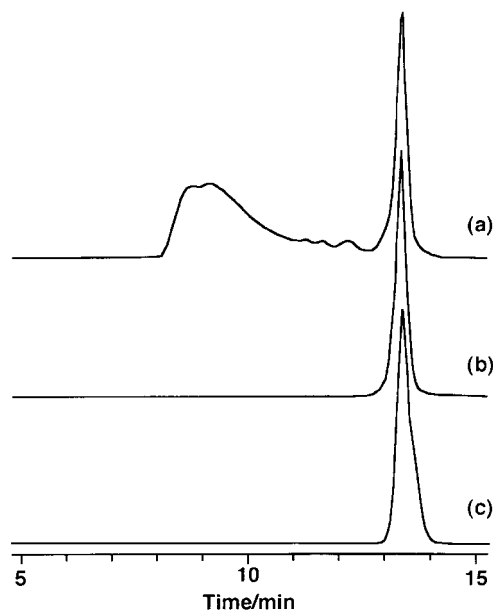


Fig. 5 Chromatogram of hydrolysis products by gel permeation chromatography. (a) hydrolysis products of DODPC liposome, which was irradiated at dose rate 1.65 kGy h⁻¹ for 5 h, (b) hydrolysis product of non-irradiated DODPC liposome, and (c) octadeca-2,4-dienoic acid. Column: G2500H_{XL}+G2000H_{XL}, range of molecular weights 3.5 × 10⁴–3 × 10².

liposome. Fig. 9 shows the change of diameter for MODPC and PODPC liposomes after freezing and thawing, for various irradiation levels. The diameters of non-irradiated MODPC and PODPC liposomes changed in all cases after a freeze-thaw cycle. After freeze-thawing of non-irradiated and short time irradiation (*e.g.*, 0.5 h) of the MODPC and PODPC liposomes, the sizes increased to around 1000–2000 nm with a wide size distribution (Fig. 9). The liposome solution became turbid due to either aggregation or fusion of the particles. The change in diameter as a function of the polymerization conversion (Fig. 10) clearly shows that the diameter of MODPC liposomes did not change significantly even for low polymerization conversion levels around 40%. For PODPC liposomes, it was difficult to stabilize the membrane of vesicles even for polymerization conversion of 60%.

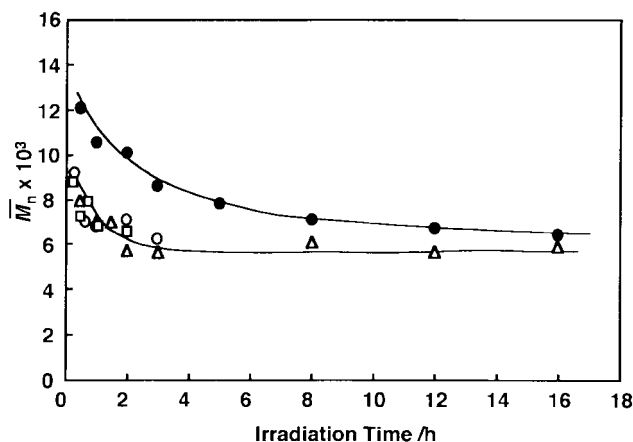


Fig. 6 Relationship between number-average molecular weight and irradiation time, for various dose rates. The number-average molecular weights were obtained from hydrolysis of irradiated DODPC liposomes. Dose rate: (●); 1.65 kGy h⁻¹, (△); 3.3 kGy h⁻¹, (○); 5.0 kGy h⁻¹, and (□); 10.0 kGy h⁻¹.

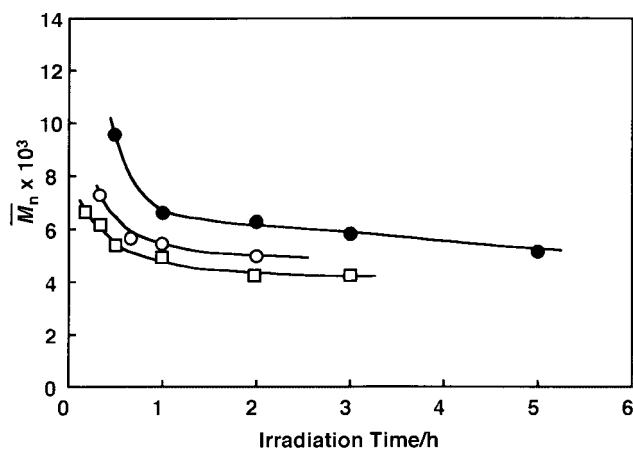


Fig. 7 Relationship between number-average molecular weight and irradiation time, for various dose rates. The number-average molecular weights were obtained from hydrolysis of irradiated SODPC liposomes. Dose rate: (●); 1.65 kGy h⁻¹, (○); 5.0 kGy h⁻¹, and (□); 10.0 kGy h⁻¹.

Discussion

Surface pressure–area isotherms

All of our synthesized polymerizable phospholipids contain the octadeca-2,4-dienoyl groups in the 2-position of glycerophosphatidylcholine units, only fatty acyl chains of the 1-acyl chains are different (*i.e.*, saturated or unsaturated, different lengths of methylene units). The monolayer of DODPC had a lower compressibility at 4 °C. On the other hand, the monolayer of SODPC was easy to compress, although the length of the 1-acyl chain in SODPC is the same as that in the DODPC molecule. The difference of compressibility between DODPC and SODPC molecules might be due to intermolecular interaction (van der Waals interaction) of the DODPC molecules, which is weaker than the intermolecular interaction between the SODPC molecules.

On the other hand, in the monolayer of monofunctional phospholipids, the ease of compression increased with increasing length of the fatty 1-acyl chains. By increasing the length of the fatty 1-acyl chains, the chain–chain interactions between neighboring molecules would increase. Regarding the effect of the fatty acyl chain, by measuring surface pressure–area isotherms and by using DSC, Ogino *et al.* reported interactions between water molecules and L- α -phosphatidylcholines, which are saturated diacylphosphatidylcholines of different acyl chain lengths (*e.g.* DMPC, DPPC, and DSPC *etc.*).²⁴ They concluded that the length of the acyl chains was affected by the film phase of the monolayer (*i.e.*, either condensed or expanded film) due to the intermolecular interaction of the acyl chains of each phosphatidylcholine. By increasing the length of the fatty acyl chain, the film changes from an expanded to a condensed film. Furthermore, they concluded that both monolayer and bilayer membranes of liposomes might experience the same horizontal intermolecular interaction by the chain–chain interaction. Although we used different phospholipids from those used in the study by Ogino *et al.*,²⁴ these findings can also be applied to our polymerizable phospholipids, which contain the polymerizable fatty acyl chain as the 2-acyl chain and different chain lengths in the 1-acyl chain (myristoyl, palmitoyl and stearoyl). Therefore, the chain–chain interaction of polymerizable phospholipids in liposomes is probably similar to the interactions of monolayers.

Polymerization of liposomes

A kinetic study was carried out for the polymerization of DODPC liposomes by γ -rays. The γ -rays cause polymerization

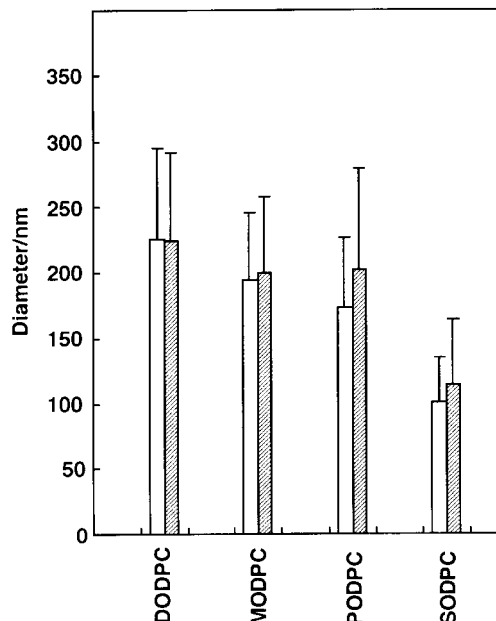
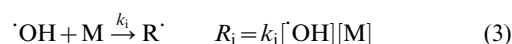
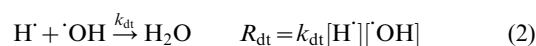
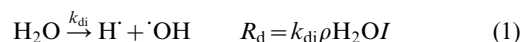


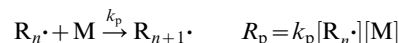
Fig. 8 Change of diameter before and after freeze–thawing for various irradiated liposomes with polymerization conversion near 50%. Error bars represent standard deviation of mean diameter for liposomes, (□) before freeze–thawing and (■) after freeze–thawing. For SODPC, the liposome was extruded through a filter of 0.1 μ m pore size.

of liposomes by creating hydroxyl radicals, which are generated when the γ -rays decompose the water surrounding the liposomes. The concentration of hydroxyl radicals during γ -irradiation remained constant. The conversion curve showed increased convexities with irradiation and molecular weight decreased gradually with irradiation (Figs. 3 and 6). From the result of the polymerization conversions, the polymerization kinetics approximate a stationary state of polymerization in which initiation is equal to termination.²⁵ This polymerization behavior was classified as a slow initiation and a stationary system.²⁶ The mechanism for γ -ray polymerization of the liposomes is presented in 4 steps as described in the following elementary reactions.²⁰

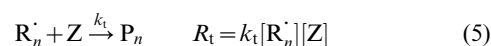
Initiation



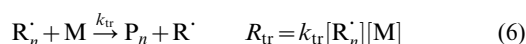
Propagation



Termination



Chain transfer



from eqns. (2) and (3)

$$[\cdot\text{OH}] = \frac{k_{\text{di}}\rho\text{H}_2\text{O}I}{k_{\text{dt}}[\text{H}^\cdot]} = KI \quad (7)$$

where

$$K = \frac{k_{\text{di}}\rho\text{H}_2\text{O}}{k_{\text{dt}}[\text{H}^\cdot]} \quad (8)$$

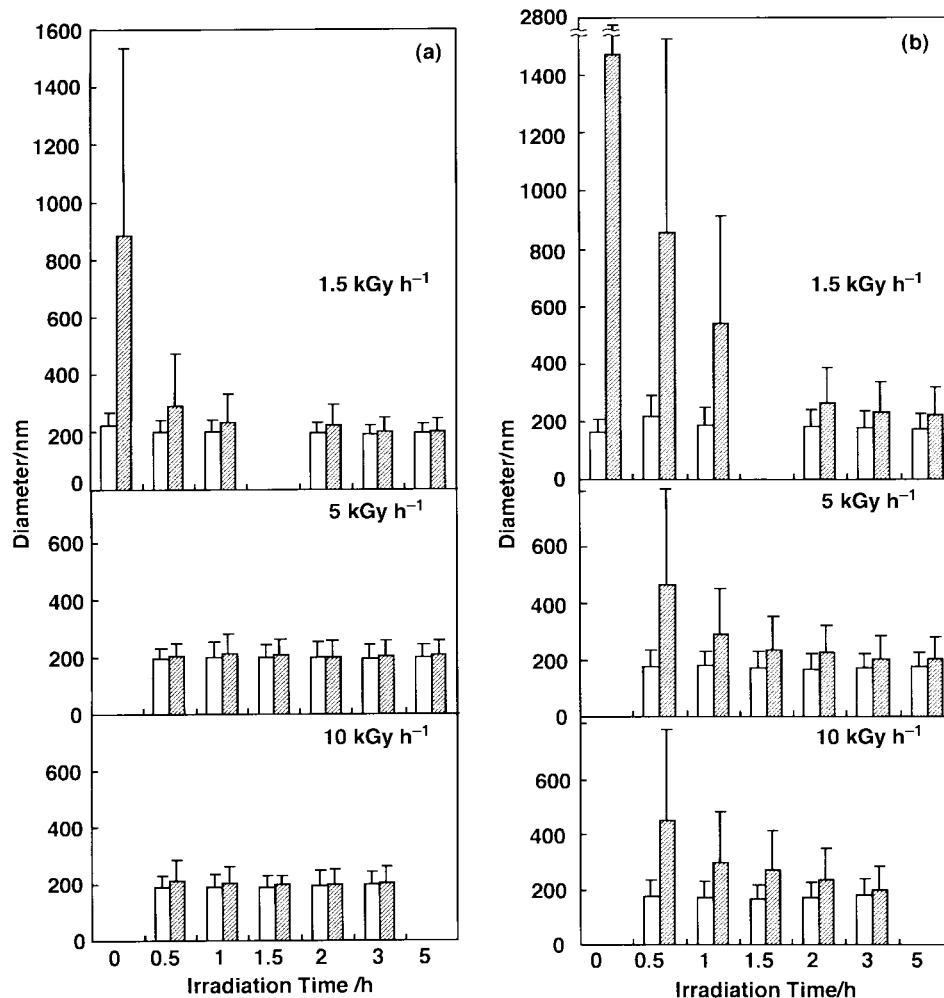


Fig. 9 Change of diameter before and after freeze-thawing for MODPC and PODPC liposomes, for various dose rates and irradiation times. Error bars represent standard deviation of mean diameter for liposomes. (a) MODPC liposome and (b) PODPC liposome; (□) before freeze-thawing and (■) after freeze-thawing.

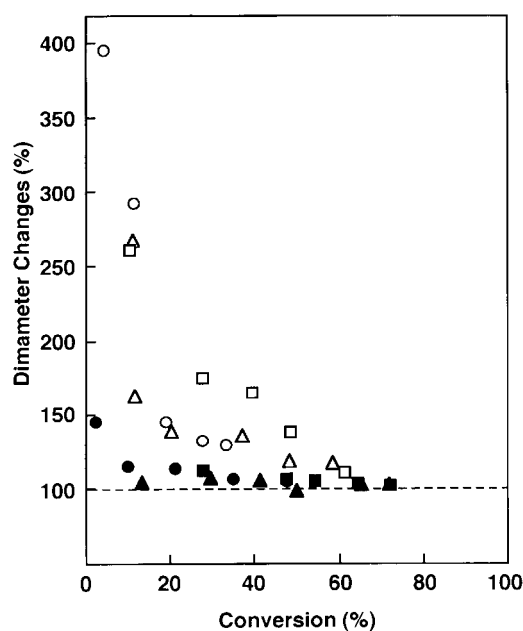


Fig. 10 Diameter changes vs. conversion for MODPC and PODPC liposomes; MODPC liposome: (●) 1.5 kGy h⁻¹, (▲) 5 kGy h⁻¹, and (■) 10 kGy h⁻¹. PODPC liposome: (○) 1.51 kGy h⁻¹, (△) 5 kGy h⁻¹, and (□) 10 kGy h⁻¹.

where M is the monomer, R' and R_n' are monomeric active and growing radicals, respectively, Z is a substance by which R_n' is deactivated. R_d , R_{dt} , R_i , R_p , R_t and R_{tr} denote the rate of radical formation from the water, its reverse reaction, initiation, propagation, termination, and chain transfer, respectively. The corresponding rate constants are denoted by k_{di} , k_{dt} , k_i , k_p , k_t and k_{tr} , respectively. ρ_{H_2O} and I are the density of water and dose rate, respectively.

For the initiation rate equal to the termination rate (*i.e.*, $R_i = R_t$), from eqns. (3), (5) and (8),

$$[R_n'] = \frac{k_i KI}{k_t [Z]} [M] \quad (9)$$

Eqn. (4) can be written by using eqn. (9) as

$$R_p = -\frac{d[M]}{dt} = k_p \frac{k_i KI}{k_t [Z]} [M]^2 \quad (10)$$

From eqn. (10), the relationship of monomer concentration and irradiation time can be expressed by eqn. (11):

$$\frac{1}{[M]_t} = -k_p \frac{k_i KI}{k_t [Z]} t + \frac{1}{[M]_0} \quad (11)$$

where $[M]_0$ and $[M]_t$ are the monomer concentration at time 0 and t , respectively.

The kinetic treatment was applied to DODPC liposome. For DODPC liposomes, the conversion curve (see Fig. 3) shows a rapid rise to 50%, followed by a slower increase. Therefore, the

reaction can be divided into two steps: reactions governing the conversion up to 50% (region I) and reactions in the region above a conversion of 50% (region II). Eqn. (11) applies to each region. For region I, the plot of the irradiation time *vs.* the inverse of the monomer concentration gave a linear relationship at various dose rates, with an intercept of 1 (Fig. 11). Region II also gave a linear relationship, with an *x*-intercept corresponding to the start time of region II.¹⁷ The slope of this line corresponds to the overall polymerization rate constant, although polymerization in reaction regions I and II proceeds independently. Fig. 13 shows the plot of the obtained overall rate constants *vs.* dose rate for each region. We found that eqns. (3)–(6) and (8) satisfied this mechanism.

Using the degree of polymerization and monomer concentration, we confirmed that this mechanism is reasonable. If the termination is first-order, the degree of polymerization can be expressed as eqn. (12):

$$\bar{P}_n = \frac{\int_0^t R_p dt}{\int_0^t R_i dt + \int_0^t R_{tr} dt} \quad (12)$$

From eqns. (4) to (6), eqn. (12) can be expressed as a function of the relationship between the degree of polymerization and the monomer concentration as eqn. (13):

$$\frac{1}{\bar{P}_n} = \frac{k_i[Z]}{k_p} \cdot \frac{1}{M_p} \int_0^t \frac{R_p}{[M]} dt + \frac{k_{tr}}{k_p} \quad (13)$$

where \bar{P}_n is the degree of polymerization, $M_p = \int_0^t R_p dt$, *i.e.*, concentration of consumed monomer at time *t*.

Fig. 12 shows plots of eqn. (13) as the inverse of the degree of polymerization *vs.* monomer concentration in each region. A linear relationship was obtained in each region, with region-dependent slope. These results can be reasonably explained by using the kinetic treatment of degree of polymerization by a two-step polymerization with different reactivities. The difference in reactivity might be explained as follows: The slope and the *y*-intercept of the lines in Fig. 12 correspond to $k_i[Z]/k_p$ and k_{tr}/k_p in eqn. (13), respectively. The slopes of the lines within each region were nearly the same, and the *y*-intercepts of all lines were also nearly the same (Fig. 12). These results show that the rate constant (k_p) in each region is nearly constant in these systems. On the other hand, the overall rate constant ($k_p k_i K / k_t [Z]$) for region II decreased by a factor about 10 from the rate constant for region I (Fig. 13). The rate of polymerization (R_p) of region II was about 10% smaller than that of region I. Inserting $k_i[Z]/k_p$ into eqn. (10), we see that the decrease of R_p in region II resulted in a decrease of k_i , because $k_i[Z]/k_p$ is constant within each region. The rate of the initiation

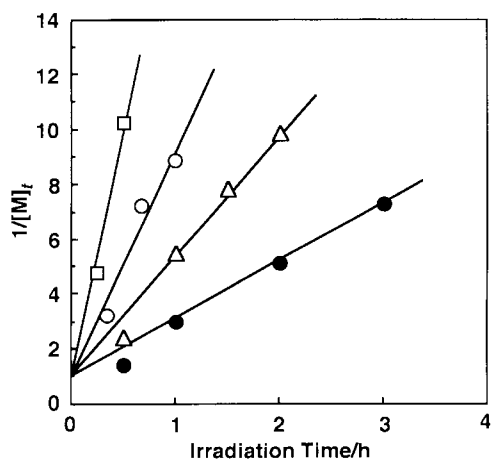


Fig. 11 Plot of $1/[M]_t$ *vs.* irradiation time for DODPC liposomes. Dose rate: (●); 1.65 kGy h⁻¹, (△); 3.3 kGy h⁻¹, (○); 5.0 kGy h⁻¹, and (□); 10.0 kGy h⁻¹.

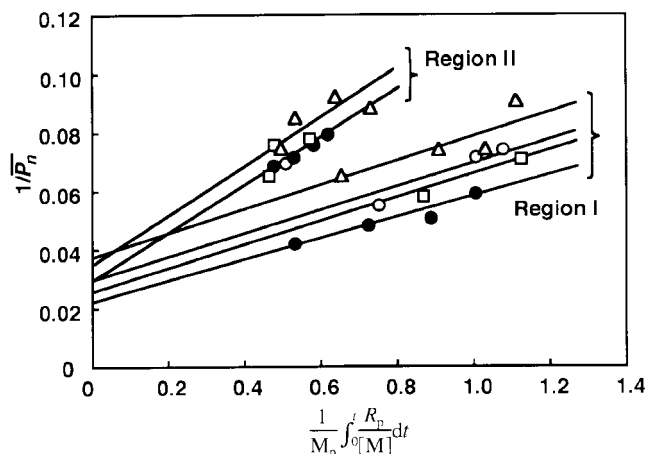


Fig. 12 Plot of inverse of degree of polymerization *vs.* $1/M_p \cdot \int_0^t (R_p/[M]) dt$ for each region of DODPC liposome. (●); 1.65 kGy h⁻¹, (△); 3.3 kGy h⁻¹, (○); 5.0 kGy h⁻¹, and (□); 10.0 kGy h⁻¹.

step in region II is smaller than that of region I. Consequently, in this system the rate of polymerization is affected by the initiation step.

The two acyl chains of phosphatidylcholine provide two different environments in bilayer membranes, such as liposomes. The diene moiety in the 2-acyl chain of DODPC might be associated with the aqueous phase. The diene moiety in the 1-acyl chain of DODPC is located in a more hydrophobic environment than that of the 2-acyl chain of DODPC. This hypothesis is demonstrated by using different radical initiators for DODPC or PODPC liposomes.^{15,16,27} During γ -ray polymerization, the 2-acyl chain on DODPC liposomes is easily attacked by the hydroxyl radical, which acts as an initiator.²⁸ The 2-acyl chain apparently polymerizes first, followed by the 1-acyl chain. The polymerization of each region proceeds independently of the other. The reason is that it is difficult for hydroxyl radicals to penetrate the diene groups

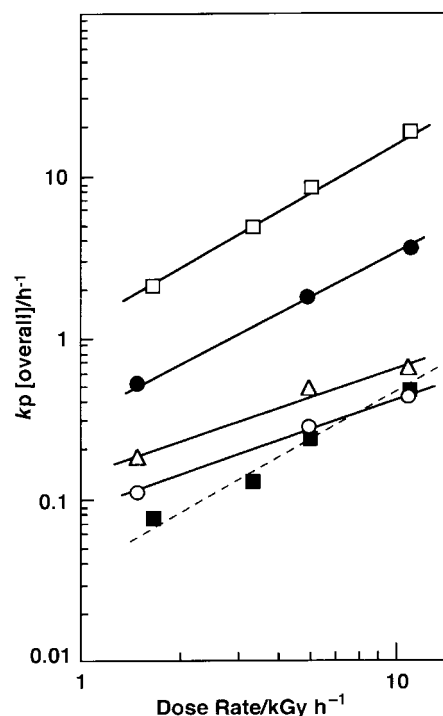


Fig. 13 Overall rate constant (k_p) *vs.* dose rates for various polymerizable liposomes. (□) DODPC liposome on region I, (●) DODPC liposome on region II, (●) SODPC liposome, (△) MODPC liposome, and (○) PODPC liposome.

of the 1-acyl chain, which is located in a hydrophobic environment. Therefore, polymerization of regions I and II corresponds to polymerization of the 2- and 1-acyl chains, respectively. Consequently, the diffusion of hydroxyl radicals is sufficiently slow that the initiation reaction of the 1-acyl chain is slower than that of the 2-acyl chain. Kinetic studies suggest that the polymerizable 1- and 2-acyl chains of DODPC liposome have different reactivities when irradiated with γ -rays. The difference can be explained by the diffusion of the hydroxyl radical being the rate-determining step during polymerization induced by γ -irradiation.

Although we used a homogeneous polymerization model to describe 2-dimensional polymerization with restricted mobility, the mechanism of polymerization is the same for both 1- and 2-acyl chains. The only difference is the value of k_i , which is a parameter of the initiation reaction. The polymerization of the octadeca-2,4-dienoyl group in the bilayer membrane proceeds by 1,4-addition, which requires conformational rearrangement before polymerization. Ringsdorf and Schupp reported polymerization of octadeca-2,4-dienoic acid in the monolayer.²⁹ The polymerization of octadeca-2,4-dienoic acid proceeds only in monolayers that are in a regular formation. This finding also applies to bilayer membranes in the liposome that consist of polymerizable phospholipids with an octadeca-2,4-dienoyl moiety. At low temperatures, such as 4 °C, the mobility of the DODPC molecules on the membrane was already restricted, but might be stacked and arranged for easy polymerization. The first stage of polymerization occurs at the 2-acyl chain, because hydroxyl radicals readily attack the 2-acyl chains that face the aqueous phase. After the initiation reaction, the rearranged molecules on the membrane easily react with 1,4-addition at the 2-acyl chain. In this case, polymerization only occurs between the 2-acyl chain and the 2-acyl chains of the neighboring molecules. It is difficult to cause either intramolecular or intermolecular polymerization between the 1- and 2-acyl chains, because the 1- and 2-acyl chains are far apart and do not rearrange to permit 1,4-addition. After the first stage of polymerization of the monolayer is completed, the 1-acyl chain of DODPC still retains its regular formation. For the second stage, 1-acyl chain polymerization, the 1-acyl chain easily rearranges to a polymerizable conformation. If the initiator attacks the diene group of the 1-acyl chain polymerized with the 2-acyl chain, polymerization occurs immediately. The activated radicals react with the neighboring molecules even without finding a polymerizable monomer. The 1-acyl chain successively polymerizes, although the rate of polymerization is slower than that of the 2-acyl chain, due to the initiation step being rate-determining. Therefore, this polymerization behavior can be explained by using a homogeneous polymerization model.

To explain the reactivity of DODPC liposomes, we synthesized non-polymerizable saturated fatty acyl chains as the 1-acyl chains and octadeca-2,4-dienoyl groups as the 2-acyl chains, by polymerization of the liposomes using γ -irradiation. 1-Stearoyl-2-[(*E,E*)-octadeca-2,4-dienoyl]-*sn*-glycero-3-phosphocholine (SODPC), which has octadeca-2,4-dienoyl groups at its 1-position and the same number of carbon atoms in each acyl chain as DODPC, was polymerized by γ -rays under the same conditions as for DODPC liposomes. The polymerization behavior of SODPC liposomes was similar to that of DODPC liposomes. Fig. 14c shows a plot of the inverse monomer concentration vs. irradiation time, and as indicated by eqn. (11), yields a straight line with a y -intercept of 1. This suggests that SODPC liposomes are polymerized by the same mechanism as DODPC liposomes.³⁰ However, the polymerization rate of SODPC liposomes decreased to 20 to 25% of the polymerization rate of DODPC liposomes (Fig. 13). This decrease in the overall rate constant ($k_p k_i KI / k_t [Z]$) of SODPC suggests a decrease in both k_p and k_i , and an increase in $k_t [Z]$ compared with DODPC liposomes. A plot of eqn. (13) as the

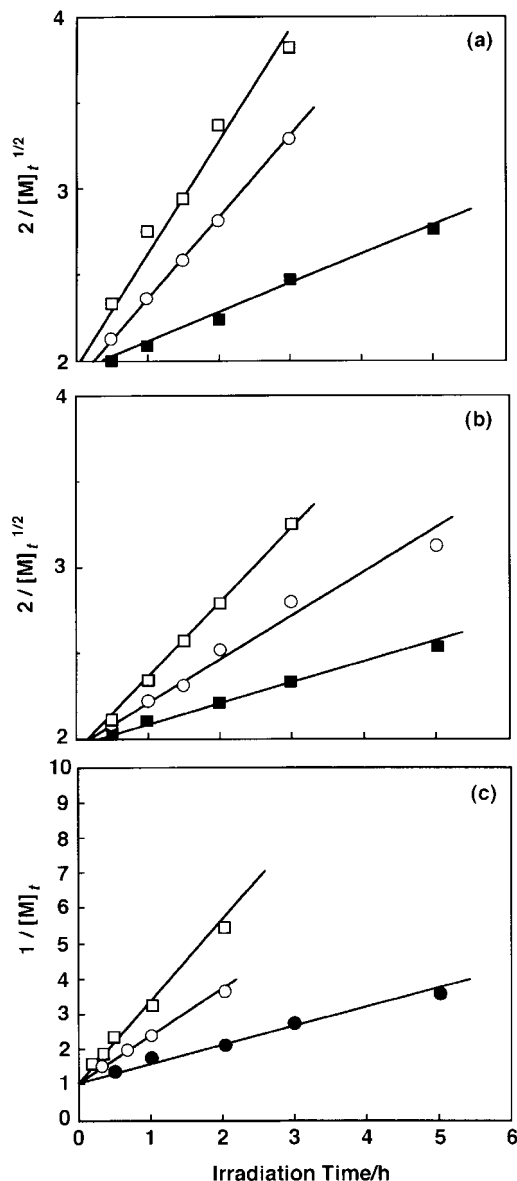
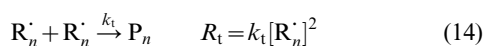


Fig. 14 Plot of $2/[M]_t^{1/2}$ vs. irradiation time. (a) MODPC liposome and (b) PODPC liposome. Dose rate: (■); 1.5 kGy h⁻¹, (○); 5.0 kGy h⁻¹, and (□); 10.0 kGy h⁻¹. (c) Plot of $1/[M]_t$ vs. irradiation time for SODPC liposome. Dose rate: (●); 1.65 kGy h⁻¹, (○); 5.0 kGy h⁻¹, and (□); 10.0 kGy h⁻¹.

inverse of the degree of polymerization vs. the monomer concentration in SODPC liposomes was linear with a slope ($k_t [Z] / k_p$) for SODPC, a two-fold increase compared with the slope for DODPC.³⁰ When $k_t [Z] / k_p$ was included in the overall rate constant ($k_p k_i KI / k_t [Z]$), the $k_i KI$ of SODPC decreased by about 50% compared with that of DODPC. Furthermore, the decrease in k_p was because the decrease in the overall rate constant was larger than the decrease in k_i . On the other hand, our results showed that because k_t is equal to k_i , k_t did not increase, but decreased in this polymerization system. Therefore, the decrease in the overall rate constant of SODPC is due to the decrease in both k_i and k_p . The difference in the polymerization rate between SODPC and DODPC might be explained as follows. The decrease in the initiation of SODPC indicated that the diene moiety of the octadeca-2,4-dienoyl group of SODPC is in a different environment from that of DODPC. The diene moiety of the 2-acyl chain of SODPC might be further from the water phase than that of DODPC, or SODPC molecules might have a somewhat denser packing than DODPC molecules. In either case it would be more difficult for

hydroxyl radicals to penetrate to the reactive diene moiety. Thus, the rate of initiation decreases due to the decrease in the diffusion of hydroxyl radicals. For the decrease in propagation, the reaction requires rearrangement of the conformation of the octadeca-2,4-dienoyl moiety because this polymerization proceeds by 1,4-addition of the octadeca-2,4-dienoyl moiety. For SODPC liposomes, it is more difficult to change the conformation of the monomer for polymerization compared with DODPC. Consequently, the rate of polymerization decreased with decreasing rates of both initiation and propagation.

On the other hand, the polymerization behavior of MODPC and PODPC liposomes differed from that of SODPC liposomes. The rates of polymerization were slower than those of SODPC liposomes. The rate of polymerization decreased in the following order (Fig. 13); SODPC > MODPC > PODPC. The molecular weight could not be measured, because of insolubility in THF. Though the rates of polymerization of MODPC and PODPC were slower than those for SODPC liposomes, the molecular weights of poly(octadeca-2,4-dienoyl acid)s, which are hydrolyzed MODPC and PODPC liposomes, were higher than that of SODPC. It is estimated that this behavior differs from that of SODPC liposomes. If termination occurs, causing recombination of the end of the chain transfer, then the termination reaction is represented by eqn. (14).



Eqn. (14) can be written by using eqns. (3), (5), and (8)

$$[R_n \cdot] = \left(\frac{k_i KI}{k_t} \right)^{1/2} [M]^{1/2} \quad (15)$$

From eqns. (4) and (15), the relationship of monomer concentration and irradiation time can be expressed by eqn. (16).

$$\frac{2}{[M]_t^{1/2}} = k_p \left(\frac{k_i KI}{k_t} \right)^{1/2} t + \frac{2}{[M]_0^{1/2}} \quad (16)$$

Fig. 14a and 14b show plots of $2/[M]^{1/2}$ vs. irradiation time, and according to eqn. (16), yield straight lines. The x -intercept of $2/[M]^{1/2}$ indicates the time of the induction period as shown from the polymerization conversion curves (Fig. 4a and 4b). Fig. 13 shows the slope of eqn. (16), which indicates the rate of polymerization, vs. the dose rate, and yields a straight line whose slope is 0.7. This suggested that for MODPC and PODPC liposomes, the termination step preferentially occurs by recombination. The intermolecular interaction of MODPC and PODPC decreases relative to that of SODPC, because the surface pressure–area isotherms of MODPC and PODPC are different from that of SODPC. The intermolecular interactions of MODPC and PODPC are also probably different from that of SODPC. This recombination–termination behavior of MODPC and PODPC liposomes is due to the decreased intermolecular interaction of neighboring molecules, which in turn increases the mobility of the monomer and growing radical. This is also suggested from results on differences in the ability of the molecules to change conformation in response to polymerization; the mobility of MODPC and PODPC molecules is greater than that of SODPC molecules. Therefore, the termination reaction prefers recombination to unimolecular termination, and the molecular weight increases over that of SODPC. Moreover, the intermolecular interaction of MODPC decrease relative to that of PODPC, so that the chain length of the 1-position of MODPC is as short as that of PODPC. The mobility of MODPC molecules in bilayer membranes is greater than that of the PODPC molecules. Therefore, the rate of polymerization of MODPC that we measured was as rapid as that of PODPC.

Stabilities of polymerized liposomes

Fig. 8 indicates that the polymerized DODPC liposomes are more stable than any other monofunctional polymerizable phospholipids. We also observed that the molecular weights of poly(octadeca-2,4-dienoyl acid)s hydrolyzed to DODPC and SODPC liposomes are similar. However, DODPC, which contains two polymerizable groups in a molecule, is cross-linked due to the polymerization of the 1-acyl chains following the polymerization of the 2-acyl chains. Consequently, the overall molecular weight was higher than the measured molecular weight. Furthermore, it is estimated that the molecular weight of poly(octadeca-2,4-dienoyl acid)s that are hydrolyzed to MODPC liposomes is as high as that of PODPC liposomes, because the stability of polymerized MODPC liposomes is higher than that of PODPC liposomes. As a control, the DPPC liposome was used to compare the stability of the liposomes for the freeze–thaw tests. The diameter of the DPPC liposome changed from 201 ± 53 nm to 234 ± 70 nm. The changes of the mean diameter of DPPC were relatively small compared with the non-polymerized, shortly irradiated (0.5 h) MODPC and PODPC liposomes (see Figs. 8 and 9). The monolayer of DPPC was a condensed film at this temperature.²⁴ The intermolecular interaction of DPPC molecules in the liposome might be stronger than those of non-irradiated MODPC and PODPC molecules in the liposomes. However, the polymerized MODPC and PODPC liposomes were more stable than the DPPC liposome during the freeze–thaw cycle.

Conclusions

The polymerization of liposomes is initiated by hydroxyl radicals generated by γ -irradiation that decomposes the water surrounding the liposome membrane surfaces. For the DODPC liposome, the two diene groups in the 1- and 2-acyl chains see different environments. That is, as Tsuchida *et al.*^{15,16,27} reported, the diene group of the 2-acyl chains might face the water phase and the diene group of the 1-acyl chains might exist in a hydrophobic environment. Kinetic studies suggest that the γ -ray polymerization of DODPC liposomes can be represented as a two-step polymerization: the 2-acyl chains are polymerized first, followed by the 1-acyl chains. The reason is that hydroxyl radicals readily attack the diene groups of the 2-acyl chain, which is located in a hydrophilic environment. Furthermore, it is difficult for hydroxyl radicals to penetrate the diene groups of the 1-acyl chain, which is located in a hydrophobic environment. The difference can be explained by the diffusion of the hydroxyl radical being the rate-determining step during polymerization induced by γ -irradiation. Therefore, DODPC liposomes containing two polymerizable groups in a molecule selectively polymerize each other even though irradiated with γ -rays. Furthermore, the polymerization behavior of SODPC liposomes with monofunctional polymerizable lipids is the same as that of DODPC liposomes. However, the fact that the initiation and propagation rates were different might be due to the decrease in hydroxyl radicals and the susceptibility of the conformational rearrangement. On the other hand, the polymerization rates of MODPC and PODPC liposomes differ from that of SODPC liposomes, which have the same polymerizable groups on the 2-acyl chains in phosphatidylcholine. The polymerized MODPC liposomes are more resistant to freeze–thaw damage than are PODPC liposomes. The termination of the MODPC and PODPC liposomes is preferable to recombination. Therefore, the molecular weight of the poly(octadeca-2,4-dienoyl acid)s polymer on hydrolysis to MODPC and PODPC liposomes might be larger than that of the SODPC liposome. In general, the polymerized liposomes consist of monofunctional polymerizable lipids that are less

stable than liposome membranes. In fact, the stability of SODPC and PODPC liposomes is lower than the stability of DODPC liposomes. The stability of irradiated MODPC liposomes, however, is similar to that of DODPC liposomes. Thus, even though polymerizable phospholipids may contain the same polymerizable groups for the 2-acyl chain, for different hydrocarbon lengths of its 1-acyl chain, different polymerization behavior and characteristics are observed for γ -ray irradiation under similar polymerization conditions (*i.e.* although the polymerization conditions using γ -irradiation are the same, the polymerization behaviour and characteristics differ for each phospholipid). The reason for this is that the mobility of the monomer and the growing chains are different among the packing and conformation of phospholipids in bilayer membranes. The packing density and conformation of phospholipids are affected by the length of the acyl chain of the phospholipids. The design of polymerizable phospholipids is therefore important for obtaining a stabilizable liposome by polymerization.

Experimental

Materials

Unless otherwise stated all reagents and chemicals (*e.g.*, diethyl ether, ethanol, methanol, tetrahydrofuran (THF), and calcium dichloride) were obtained commercially and used without further purification. 4-Dimethylaminopyridine (DMAP) and *N,N'*-dicyclohexylcarbodiimide (DCC) were obtained from Wako Pure Chemical Industries, Ltd.; and 1,2-dimyristoyl-*sn*-glycero-3-phosphocholine (DMPC), 1,2-dipalmitoyl-*sn*-glycero-3-phosphocholine (DPPC) and 1,2-distearoyl-*sn*-glycero-3-phosphocholine (DSPC) were obtained from NOF Corporation. Chloroform was distilled with phosphorus pentoxide before use in order to remove alcohol. Reagent-grade methanol and chloroform were used as eluents without further purification. Ultra-pure water was purified with a TORAYPURE LV-08 system (TORAY Co., Ltd.). Other materials used were ion-exchange resin (AMBERLITE[®] IRC-50, Organo Co., Ltd.), silica gel (C-200, Wako Pure Chemical Industries, Ltd.), and thin layer chromatography (TLC) plates (Silica gel 60 F254, Merck).

Phospholipase A₂ was purified by heating 19 mg of Snake Venom (from *Naja naja kaouthia*, Wako Pure Chemical Industries, Ltd.) in 10 mL of acetic acid buffer (CH₃COOH–CH₃COONa, pH 5.0) at 90 °C for 5 min. The mixture was then allowed to stand at room temperature for 30 min, and then centrifuged at 3000 rpm for 5 min. The upper layer of the centrifuge tube was used for the phospholipase A₂ solution.

The (*E,E*)-octadeca-2,4-dienoic acid was synthesized as follows. Ethyl octadeca-2,4-dienoate was prepared by coupling triethyl 4-phosphonocrotonate with tetradecanal by using the Wittig reaction. The ester was hydrolyzed, and the precipitate was recrystallized twice from *n*-hexane. L- α -Glycerophosphorylcholine (GPC) was obtained from egg yolk lecithin by the method of Hanahan.³¹

(*E,E*)-Octadeca-2,4-dienoic anhydride 1

A solution of 100 g of (*E,E*)-octadeca-2,4-dienoic acid (0.3566 mol) in 500 mL of chloroform was placed in a 1 L round-bottomed flask equipped with a dropping funnel and nitrogen bubbler, and stirred mechanically at 4 °C for an hour under a nitrogen atmosphere. To the mixture was added dropwise 44.1 g of DCC (0.2140 mol) dissolved in 50 mL of chloroform within 10 min at 4 °C, and then the reaction mixture was stirred at room temperature for 2 h. After the reaction, precipitated dicyclohexylurea was filtered off under vacuum, then the precipitate was washed twice with 50 mL of cold chloroform. The filtrates were combined, and the solution

of (*E,E*)-octadeca-2,4-dienoic anhydride was used without further purification in the next acylation reaction.

1,2-Bis[*(E,E)*-octadeca-2,4-dienoyl]-*sn*-glycero-3-phosphocholine (DODPC) 2

L- α -Glycerophosphorylcholine (16.5 g, 64.15 mmol) was dried twice by evaporation of dry benzene. A solution of (*E,E*)-octadeca-2,4-dienoic anhydride (*ca.* 17.83 mmol) and 11 g of DMAP (90.04 mmol) were added and stirred mechanically for 2 days at 30 °C under a nitrogen atmosphere. The progress of the reaction was monitored by TLC (CHCl₃–MeOH–H₂O=65:25:4). After the reaction, the solvent was evaporated *in vacuo* below 30 °C. The residue was chromatographed on 650 g of silica gel with eluted CHCl₃–MeOH gradient solvents (10:0, 9:1, 8:2, 7:3, 5:5) using an open column (*i.d.* of 10 cm). The elute-containing PC fraction was combined and the solutions evaporated. The residue was purified by using a middle-pressure chromatograph on 100 g of silica gel (*i.d.* of 30 mm, length of 22 cm, elute was CHCl₃–MeOH–H₂O=80:19:1, 80:18:2, pressure was 0.2 kgf cm⁻², flow rate was 35 mL min⁻¹, pump was Model-540 Yamazen). The elute was passed through a column of ion-exchange resin to remove the residual DMAP. The resin was washed with 1 L of the MeOH and CHCl₃ before use. The combined eluents were evaporated and the residue was suspended in 200 mL of ultra-pure water. The suspension was frozen by liquid nitrogen and the solid was freeze-dried *in vacuo* for 24 h. The pure DODPC was obtained in 28.9% yield (14.5 g, 18.54 mmol): *R*_f=0.2 (CHCl₃–MeOH–H₂O=65:25:4); ¹H NMR (CDCl₃) δ 0.88 (t, *J*=6.6 Hz, 6 H, CH₃), 1.20–1.35 (m, 40 H, CH₂), 1.35–1.50 (m, 4 H, CH₂CH₂C=C), 2.15 (s, 4H, CH₂C=C), 3.32 (s, 9 H, N(CH₃)₃), 3.75 (s, 2 H, CH₂N), 4.01 (m, 2 H, CH₂OCO), 4.20–4.50 (m, 4 H, CH₂CH₂N, CH₂OCO), 5.22–5.35 (m, 1 H, CHOCO), 5.74 and 5.76 (d, *J*=15 Hz, 2 H, C=CHCOO), 6.10–6.20 (m, 4 H, CH₂CH=CH), 7.15–7.30 (m, 2 H, CH=CCOO); ¹³C NMR (CDCl₃) δ 13.99, 22.56, 28.64, 29.19, 29.25, 29.37, 29.50, 29.57, 31.82, 32.97, 54.28, 59.20, 62.96, 63.41, 66.19, 70.74, 118.37, 118.50, 128.13, 145.20, 145.43, 145.74, 145.96, 166.39, 166.78; IR (KBr) 3397.1 (ν OH), 2923.5 (ν_{as} CH₂), 2853.1 (ν_s CH₂), 1716.9 (ν C=O unsat), 1644.5 (ω_{as} C=C), 1468.0 (δ_{as} CH₂), 1248.1 (ν P=O), 1091.8 and 825.6 (ν P–O), 997.3, 969.4, 723.4 cm⁻¹.

1-Myristoyl-2-[(*E,E*)-octadeca-2,4-dienoyl]-*sn*-glycero-3-phosphocholine (MODPC) 3

Into 2 L flasks was placed DMPC (45 g, 66.38 mmol) in 600 mL of Et₂O–EtOH (95:5), 300 mL of 100 mM Tris–HCl buffer (pH 8.0), 100 mL of 100 mM CaCl₂, and 15 mL of the phospholipase A₂ solution. The reaction mixture was suspended and stirred at room temperature for 19 h. The progress of the reaction was monitored by TLC (CHCl₃–MeOH–H₂O=65:25:4). Upon completion of the reaction, the solvent was evaporated under reduced pressure. The residual water phase was combined, and extracted three times with 500 mL of chloroform. To the water phase was added 500 mL of chloroform and 100 mL of methanol and the organic phase was separated; this procedure was repeated three times. Finally, the water phase was extracted three times with 500 mL of chloroform. The combined organic phase (*ca.* 4.5 L) was dried over 150 g of anhydrous Na₂SO₄ and evaporated. The residue was dried seven times by evaporation of 100 mL of dry benzene. The residue was purified by chromatography on 650 g silica gel eluted with CHCl₃–MeOH gradient solvents (10:0, 9:1, 8:2, 7:3, 5:5). The *R*_f 0.07 (CHCl₃–MeOH–H₂O=65:25:4) fractions were collected and evaporated. The pure lysomyristoyl phosphatidylcholine gave a 78.6% yield (48.8 g, 0.1043 mol). The TLC (CHCl₃–MeOH–H₂O=65:25:4) showed one spot (*R*_f 0.07).

In a 1 L flask was placed 66 wt% of (*E,E*)-octadeca-2,4-dienoic anhydride solution (*ca.* 0.1177 mol). Lysomyristoyl phosphatidylcholine (40.5 g, 86.66 mmol) and 8.44 g of DMAP (69.08 mmol) were added, and the gas in the reaction flask was replaced with nitrogen and the flask sealed. The reaction mixture was stirred for 2 days at 30 °C. The progress of the reaction was monitored by TLC (CHCl₃-MeOH-H₂O=65:25:4). After the reaction, the solvent was evaporated *in vacuo*. The residue was divided into two portions, then each portion was chromatographed on 650 g silica gel with eluted CHCl₃-MeOH gradient (10:0, 9:1, 8:2, 7:3, 5:5) using an open column (i.d. of 10 cm). The combined eluate of the *R_f* 0.2 fractions of TLC was evaporated. The residue was purified on 100 g silica gel with eluted CHCl₃-MeOH-H₂O gradient (80:19:1, 80:18:2) by using medium-pressure chromatography (i.d. of 30 mm, length of 22 cm, eluent was CHCl₃-MeOH-H₂O=80:19:1, 80:18:2, pressure was 0.2 kgf cm⁻², flow rate was 35 mL min⁻¹, pump was Model-540 Yamazen). The eluate was poured through a column of ion-exchange resin to remove the DMAP. The resin was washed with 1 L of the MeOH and CHCl₃ before use. The combined eluates were evaporated, and the residue was suspended in 200 mL of ultra-pure water. The suspension was frozen by liquid nitrogen at -196 °C, and the solid was freeze-dried *in vacuo* for 24 h. The pure MODPC gave a 39.5% yield (25 g, 34.24 mmol): *R_f*=0.19 (CHCl₃-MeOH-H₂O=65:25:4); ¹H NMR (CDCl₃) δ 0.88 (t, *J*=6.6 Hz, 6 H, CH₃), 1.00–1.35 (m, 40 H, CH₂), 1.35–1.50 (m, 2 H, CH₂CH₂C=C), 1.50–1.60 (m, 2 H, CH₂CH₂COO), 2.10–2.20 (m, 2 H, CH₂C=C), 2.27 (t, *J*=7 Hz, 2 H, -CH₂CH₂COO), 3.35 (s, 9 H, N(CH₃)₃), 3.80 (s, 2 H, CH₂N), 3.90–4.10 (m, 2 H, CH₂OCO), 4.15–4.48 (m, 4 H, CH₂CH₂N, CH₂OCO), 5.26–5.28 (m, 1 H, CHOCO), 5.75 (d, *J*=15 Hz, 1 H, C=CHCOO), 6.15 (m, 2 H, CH₂-CH=CH), 7.18–7.30 (m, 1 H, CH=CCOO); ¹³C NMR (CDCl₃) δ 14.10, 22.69, 24.92, 28.75, 29.16, 29.33, 29.49, 29.52, 29.61, 29.69, 31.93, 33.10, 34.16, 54.48, 59.28, 59.35, 63.02, 63.50, 66.47, 70.65, 70.76, 118.54, 128.19, 145.67, 146.09, 166.50, 173.58; IR (KBr) 3397 (νOH), 2955.3, 2917.7 (ν_{as}CH₂), 2850.2 (ν_sCH₂), 1735.2 (νC=O sat), 1713.9 (νC=O unsat), 1645.5 (ω_{as}C=C-C=C), 1472.8 (δ_{as}CH₂), 1262.6 (νP=O), 1092.8, 1065.8 and 832 (νP=O), 1169.0, 1008.9, 971.3, 720.5 cm⁻¹. Anal. Calcd for C₄₀H₇₆O₈PN·H₂O (748.00): C, 64.22; H, 10.51; N, 1.87. Found: C, 63.97; H, 10.76; N, 1.53%. MS (FAB): *m/z* 731 (M+1).

1-Palmitoyl-2-[(*E,E*)-octadeca-2,4-dienoyl]-*sn*-glycero-3-phosphocholine (PODPC) 4

Into a 2 L flask was placed DPPC (50 g, 68.12 mmol) in 530 mL of Et₂O-EtOH (95:5), 300 mL of 100 mM Tris-HCl buffer (pH 8.0), 100 mL of 100 mM CaCl₂, and 5 mL of the phospholipase A₂ solution. The reaction mixture was suspended and stirred at room temperature for 7 h. The progress of the reaction was monitored by TLC (CHCl₃-MeOH-H₂O=65:25:4). Upon completion of the reaction, the solvent was evaporated under reduced pressure. The residual water phase was extracted three times with 250 mL of chloroform. To the water phase was added 250 mL of chloroform and 50 mL of methanol and the organic phase was separated; this procedure was repeated three times. Finally, the water phase was extracted three times with 250 mL of chloroform. The combined organic phases (*ca.* 2 L) were dried over 70 g of anhydrous Na₂SO₄ and evaporated. The residue was dried seven times by evaporation of 100 mL of dry benzene. The residue was purified by chromatography on 650 g silica gel eluted with CHCl₃-MeOH gradient solvents (10:0, 9:1, 8:2, 7:3, 5:5). The *R_f* 0.07 (CHCl₃-MeOH-H₂O=65:25:4) fractions were collected and evaporated. The pure lysopalmitoyl phosphatidylcholine gave a 77.0% yield (26.0 g,

52.16 mmol). The TLC (CHCl₃-MeOH-H₂O=65:25:4) showed one spot (*R_f* 0.07).

In a 1 L flask was placed 44 wt% of (*E,E*)-octadeca-2,4-dienoic anhydride solution (*ca.* 78.50 mmol). Lysopalmitoyl phosphatidylcholine (20.8 g, 41.79 mmol) and 6.38 g of DMAP (52.20 mmol) were added, and the gas in the reaction flask was replaced with nitrogen and the flask sealed. The reaction mixture was stirred for 3 days at 30 °C. The progress of the reaction was monitored by TLC (CHCl₃-MeOH-H₂O=65:25:4). After the reaction, the solvent was evaporated *in vacuo*. The residue was chromatographed on 650 g silica gel with eluted CHCl₃-MeOH gradient (10:0, 9:1, 8:2, 7:3, 5:5) by using an open column (i.d. of 10 cm). The combined eluate of the *R_f* 0.2 fractions by TLC were evaporated. The residue was purified on 100 g silica gel with eluted CHCl₃-MeOH-H₂O gradient (80:19:1, 80:18:2) by using medium-pressure chromatography (i.d. of 30 mm, length of 22 cm, eluent was CHCl₃-MeOH-H₂O=80:19:1, 80:18:2, pressure was 0.2 kgf cm⁻², flow rate was 35 mL min⁻¹, pump was Model-540 Yamazen). The elute was poured through a column of ion-exchange resin to remove the DMAP. The resin was washed with 1 L of the MeOH and CHCl₃ before use. The combined eluates were evaporated, and the residue was suspended in 200 mL of ultra-pure water. The suspension was frozen by liquid nitrogen at -196 °C, and the solid was freeze-dried *in vacuo* for 24 h. The pure PODPC was obtained in 62.8% yield (20 g, 26.38 mmol): *R_f*=0.19 (CHCl₃-MeOH-H₂O=65:25:4); ¹H NMR (CDCl₃) δ 0.88 (t, *J*=6.6 Hz, 6 H, CH₃), 1.00–1.40 (m, 44 H, CH₂), 1.40–1.50 (m, 2 H, CH₂CH₂C=C), 1.50–1.65 (m, 2 H, CH₂CH₂COO), 2.10–2.20 (m, 2 H, CH₂C=C), 2.27 (t, *J*=6.6 Hz, 2 H, CH₂CH₂COO), 3.31 (s, 9 H, N(CH₃)₃), 3.80 (s, 2 H, CH₂N), 3.70–3.83 (m, 2 H, CH₂OCO), 4.15–4.45 (m, 4 H, CH₂CH₂N, CH₂OCO), 5.20–5.32 (m, 1 H, CHOCO), 5.75 (d, *J*=15.5 Hz, 1 H, C=CHCOO), 6.15 (2 H, CH₂CH=CH), 7.18–7.30 (m, 1 H, CH=CCOO); ¹³C NMR (CDCl₃) 14.12, 22.71, 24.94, 28.81, 29.2, 29.40, 29.52, 29.60, 29.72, 29.76, 31.95, 33.14, 34.18, 54.36, 59.33, 59.41, 63.05, 63.50, 63.58, 66.27, 70.62, 70.73, 118.54, 128.21, 145.68, 146.16, 166.52, 173.62; IR (KBr) 2918.7 (ν_{as}CH₂), 2850.2 (ν_sCH₂), 1735.2 (νC=O sat), 1715.9 (νC=O unsat), 1643.6 (ω_{as}C=C-C=C), 1467.0 (δ_{as}CH₂), 1257.7 (νP=O), 1089.9 and 1062.9 and 826 (νP=O), 1003.1, 969.4, 721.5 cm⁻¹. Anal. Calcd for C₄₂H₈₀O₈PN·1.5H₂O (785.06): C, 64.52; H, 10.66; N, 1.78. Found: C, 64.30; H, 10.95; N, 1.50%. MS (FAB): *m/z* 758 (M+1).

1-Stearoyl-2-[(*E,E*)-octadeca-2,4-dienoyl]-*sn*-glycero-3-phosphocholine (SODPC) 5

Into a 2 L flask was placed DSPC (50 g, 63.28 mmol) in 680 mL of Et₂O-EtOH (95:5), 340 mL of 100 mM Tris-HCl buffer (pH 8.0), 100 mL of 100 mM CaCl₂, and 17 mL of the phospholipase A₂ solution. The reaction mixture was suspended and stirred at room temperature for 19 h. The progress of the reaction was monitored by TLC (CHCl₃-MeOH-H₂O=65:25:4). Upon completion of the reaction, the solvent was evaporated under reduced pressure. The residual water phase was extracted three times with 250 mL of chloroform. To the water phase was added 250 mL of chloroform and 50 mL of methanol and the organic phase was separated; and this procedure was repeated three times. Finally, the water phase was extracted three times with 250 mL of chloroform. The combined organic phases (*ca.* 2 L) were dried over 70 g of anhydrous Na₂SO₄ and evaporated. The residue was dried seven times by evaporation of 100 mL of dry benzene. The residue was purified by chromatography on 650 g silica gel eluted with CHCl₃-MeOH gradient solvents (10:0, 9:1, 8:2, 7:3, 5:5). The *R_f* 0.07 (CHCl₃-MeOH-H₂O=65:25:4) fractions were collected and evaporated. The pure lysostearoyl phosphatidylcholine was obtained in 77.5% yield (25.6 g,

52.6 mmol). The TLC ($\text{CHCl}_3\text{-MeOH-H}_2\text{O}=65:25:4$) showed one spot (R_f 0.07).

In a 1 L flask was placed 34 wt% of (*E,E*)-octadeca-2,4-dienoic anhydride solution (*ca.* 60.62 mmol). Lysostearoyl phosphatidylcholine (25.6 g, 48.86 mmol) and 4.76 g of DMAP (38.96 mmol) were added, and the gas in the reaction flask was replaced with nitrogen and the flask sealed. The reaction mixture was stirred for 7 days at 30 °C. The progress of the reaction was monitored by TLC ($\text{CHCl}_3\text{-MeOH-H}_2\text{O}=65:25:4$). After the reaction, the solvent was evaporated *in vacuo*. The residue was chromatographed on 650 g silica gel eluted with $\text{CHCl}_3\text{-MeOH}$ gradient (10:0, 9:1, 8:2, 7:3, 5:5) by using an open column (*i.d.* of 10 cm). The combined eluate of the R_f 0.2 fractions of TLC was evaporated. The residue was purified on 100 g silica gel with eluted $\text{CHCl}_3\text{-MeOH-H}_2\text{O}$ gradient (80:19:1, 80:18:2) by using medium-pressure chromatography (*i.d.* of 30 mm, length of 22 cm, eluate was $\text{CHCl}_3\text{-MeOH-H}_2\text{O}=80:19:1, 80:18:2$, pressure was 0.2 kgf cm^{-2} , flow rate was 35 mL min^{-1} , pump was Model-540 Yamazen). The eluate was poured through a column of ion-exchange resin to remove DMAP. The resin was washed with 1 L of the MeOH and CHCl_3 before use. The combined eluates were evaporated, and the residue was suspended in 200 mL of ultra-pure water. The suspension was frozen by liquid nitrogen at -196°C , and the solid was freeze-dried *in vacuo* for 24 h. The pure SODPC was obtained in 52.0% yield (20 g, 25.44 mmol): $R_f=0.19$ ($\text{CHCl}_3\text{-MeOH-H}_2\text{O}=65:25:4$); $^1\text{H NMR}$ (CDCl_3) δ 0.88 (t, $J=6.6 \text{ Hz}$, 6 H, CH_3), 1.00–1.35 (m, 48 H, CH_2), 1.35–1.50 (m, 2 H, $\text{CH}_2\text{CH}_2\text{C}=\text{C}$), 1.50–1.65 (m, 2 H, $\text{CH}_2\text{CH}_2\text{COO}$), 2.10–2.20 (m, 2 H, $\text{CH}_2\text{C}=\text{C}$), 2.27 (t, $J=7 \text{ Hz}$, 2 H, $\text{CH}_2\text{CH}_2\text{COO}$), 3.35 (s, 9 H, $\text{N}(\text{CH}_3)_3$), 3.66–3.90 (s, 2 H, CH_2N), 3.90–4.10 (m, 2 H, CH_2OCO), 4.18–4.43 (m, 4 H, $\text{CH}_2\text{CH}_2\text{N}$, CH_2OCO), 5.22–5.30 (m, 1 H, CHOCO), 5.75 (d, $J=15.5 \text{ Hz}$, 1 H, $\text{C}=\text{CHCOO}$), 6.15 (m, 2 H, $\text{CH}_2\text{CH}=\text{CH}$), 7.18–7.30 (m, 1 H, $\text{CH}=\text{CCOO}$); $^{13}\text{C NMR}$ (CDCl_3) 14.12, 22.71, 24.94, 28.77, 29.2, 29.38, 29.51, 29.56, 29.63, 29.74, 31.95, 33.12, 34.18, 54.43, 59.32, 59.37, 63.01, 63.50, 66.32, 66.43, 70.78, 70.78, 118.54, 128.21, 145.71, 146.13, 166.50, 173.58; IR (KBr) 3413.5 (ν_{OH}), 2919.6 ($\nu_{\text{as}}\text{CH}_2$), 2851.1 ($\nu_{\text{s}}\text{CH}_2$), 1735.2 ($\nu_{\text{C}=\text{O}} \text{ sat}$), 1718.8 ($\nu_{\text{C}=\text{O}} \text{ unsat}$), 1642.6 ($\omega_{\text{as}}\text{C}=\text{CC}=\text{C}$), 1468.0 ($\delta_{\text{as}}\text{CH}_2$), 1252.0 ($\nu_{\text{P}=\text{O}}$), 1092.8 and 1065.8 and 823.7 ($\nu_{\text{P}=\text{O}}$), 970.3, 721.5 cm^{-1} . Anal. Calcd for $\text{C}_{44}\text{H}_{84}\text{O}_8\text{PN}\cdot 1.5\text{H}_2\text{O}$ (795.12): C, 64.99; H, 10.78; N, 1.72. Found: C, 65.27; H, 11.19; N, 1.42%. MS (FAB): m/z 786 ($\text{M}+1$).

Methods

Measurement. Infrared spectra were obtained with a JASCO FT/IR-7300 spectrometer. Nuclear magnetic resonance spectra (NMR) were recorded with a JEOL JNM-EX270 (270 MHz) spectrometer. The chemical shifts are given in parts per million (ppm) relative to tetramethylsilane as an internal standard. Mass spectra were obtained with a JEOL DIMS- spectrometer. Elemental analyses were performed by Ibaraki Environment Research Center, Inc.

Surface pressure–area isotherm. The surface pressure–area isotherms of polymerizable phospholipids were measured by a Wilhelmy plate method using a moving-wall type Langmuir–Blodgett membrane trough (Nippon Laser Electric). The trough dimensions were 400 mm \times 26 mm. For the subphase we used ultra-pure water, which has a resistivity of 18 M Ω . A chloroform solution of the lipids (0.7 mg mL^{-1}) was spread on the water surface using a microsyringe, and the solvent was allowed to evaporate for 20 min. The temperature of the subphase was maintained at 3.8 °C. The monolayer was compressed at a rate of $13.0 \text{ cm}^2 \text{ min}^{-1}$ (50 mm min^{-1}).

Preparation of liposomes. All of the liposomes in this study were prepared by an extrusion method according to the following procedure. Lipids (2 g) were added to a polyethylene bag (100 \times 150 cm) and hydrated with 40 mL of ultra-pure water. The dispersions were kept at a temperature above the phase transition temperature (T_c) of each phospholipid. The dispersions were homogenized by using a Stomacher (UAC HOUSE, Model: BA6020, SEWARD MEDICAL) for 20 min. The solutions were extruded stepwise through polycarbonate filters with pore size of 5, 1, 0.8, 0.4, and 0.2 mm. To reduce the diameter distribution, the liposomes were passed three times through the 0.2 mm polycarbonate filters. The liposomes were adjusted to 1.8–2.0 wt% lipid concentration by diluting with ultra-pure water.

Measurement of diameter. In a 1 cm quartz cuvette equipped with a Teflon stopper was placed 3 mL of ultra-pure water that was filtered through a 0.2 mm filter by using a syringe. The liposome solution (*ca.* 1 mL) was added, and the solution was dispersed homogeneously. The average diameter of the liposomes was measured by using a Nicomp model-370HPL particle sizer instrument (Pacific Scientific) with a He–Ne laser light source. The intensity of scattered light was recorded and converted to size distributions as a gaussian mode. The standard deviation (SD) of the mean diameter was also recorded as the scattered-light intensity.

Differential scanning calorimetry (DSC). The liposomes (60 mL, 20 mg mL^{-1} lipid concentration) were placed in large silver pans and the pans were sealed tightly. The phase transition temperatures of the liposomes were measured with a DSC-120 instrument (Seiko Instrument Inc.) at a heating rate of 1°C min^{-1} .

Polymerization of liposomes. Into a 110 mL glass vial were placed 100 mL of the 2 wt% liposomal solution, and the vials were sealed with an aluminium-covered rubber cap. Then, the solution was bubbled with argon for 30 min at room temperature. Using a 10 mL injection syringe, 5 mL of liposomal solution was transferred to a 10 mL sealed glass vial that contained an argon atmosphere. The liposomal solutions were stirred magnetically at 4 °C and irradiated with γ -rays from a ^{60}Co source (25 000 Ci). The dose rate was adjusted between 0.5 to 10 kGy h^{-1} by varying the distance between the ^{60}Co source and the liposomal solution. Fresh liposomal solutions were prepared for each measurement.

Measurement of polymerization conversion. No description of detailed method for measuring the polymerization conversion of the polymerized liposome (*e.g.*, DODPC,¹⁷ PODPC²² *etc.*) has been reported in the open literature. The baseline (*i.e.*, 100% polymerization) might be estimated by using a freehand drawing. We developed a method for drawing these polymerizable phospholipids by using simple UV-irradiation in a cell.

The monomeric liposomal solutions (DODPC liposome 14 μL , other liposomes 28 μL) were diluted with 10 mL of ultra-pure water by using a transfer pipette. The solution was dispersed homogeneously and transferred to a 1 cm quartz cell. Using a UV spectrometer (UV-240, Shimadzu Corporation), the diluted solutions were measured at room temperature for the absorption of each liposome at the absorption maximum (λ_{max}) (DODPC 254 nm, MODPC and PODPC 259 nm, SODPC 253 nm), based on the diene group. The irradiated liposomal solutions were measured by the same procedure. A polymerization yield of 100% was obtained by the following procedure: The diluted monomeric liposome was irradiated by a UV lamp (MODEL ENF-260C/J, Spectronics Corporation) at 254 nm until absorption at λ_{max} disappeared. The polymerization conversions were calculated from the difference between the absorption of the irradiated liposome solution at

λ_{\max} and that of the monomeric liposome. The polymerization conversions were calculated from eqn. (17).

$$\text{Polymerisation conversion (\%)} = (A_1 - A_T) / (A_1 - A_0) \times 100 \quad (17)$$

where A_T is the absorption intensity at λ_{\max} after irradiation, A_1 is the absorption intensity at λ_{\max} before irradiation, A_0 is the absorption intensity for 100% polymerized by UV irradiation.

Molecular weight measurement. The molecular weights of the poly(phospholipid) were determined by measuring the octadecadienoic acid polymer obtained from hydrolysis of the irradiated liposome, because the polymerized liposome was insoluble in organic solvents. To 5 mL of irradiated liposomes was added 5 mL of 2 M NaOH and the temperature of the mixture was maintained at 70 °C for 24 h. The reaction mixture was cooled to room temperature, neutralized with 5 mL of 2 M HCl, and further cooled to 4 °C. The precipitate was filtered through a 5G glass filter, washed with water, and dried *in vacuo* for 12 h. The obtained solids (10 mg) were dissolved in 5 mL of THF. The solutions containing octadecadienoic acid polymer (10 μ L) were measured by using gel permeation chromatography (HLC-802A and HLC-802UR, column: G2500H_{XL} + G2000H_{XL} and G5000H_{XL} + G3000H_{XL}, range of molecular weight 3.5×10^4 – 3×10^2 and 2×10^5 – 1×10^3 , respectively, Toyo Soda Co., Ltd.) with THF as eluent at a flow rate of 1 mL min⁻¹ at 40 °C. The molecular weights were calculated from the calibration curve by using standard polystyrenes.

Physical stability of liposomes (freeze–thawing test). To measure the stability of liposomes, a freeze–thaw test was used as follows. First, the irradiated liposome solution (2 mL) was transferred to a 10 mL sample tube and frozen with liquid nitrogen for 5 min. Then the frozen liposome was thawed gradually at room temperature. After the sample was completely thawed, the average diameters of the liposome were measured by using the same particle sizer instrument previously described. The changes in average diameter were calculated by comparing the diameter measurements taken before freezing with those taken after the freeze–thaw cycle.

Acknowledgements

The authors wish to thank Dr Yoshishige Murata and Mr Yoshio Nakano (Tsukuba Research Laboratory, NOF Corporation) for their helpful discussions and encouragement. We express deepest condolences and gratefully acknowledge Mr Fumio Hosoi, who died on March 13, 1998.

References

- 1 J. H. Fendler, *Acc. Chem. Res.*, 1980, **13**, 7.
- 2 F. C. Szoka and D. Papahadjopoulos, in *Liposomes*, ed. C. G. Knight, Elsevier, Amsterdam, 1981, p. 51.
- 3 E. Mayhew and D. Papahadjopoulos, in *Liposomes*, ed. M. J. Ostro, Marcel Dekker, Inc., New York, 1983, p. 289.
- 4 H. Ringsdorf, B. Schlarb and J. Venzmer, *Angew. Chem., Int. Ed. Engl.*, 1988, **27**, 113.
- 5 B. Hupfer, H. Ringsdorf and H. Schupp, *Chem. Phys. Lipids*, 1983, **33**, 355.
- 6 D. S. Johnston, L. R. McLean, M. A. Whittam, A. D. Clark and D. Chapman, *Biochemistry*, 1983, **22**, 3194.
- 7 K. Dorn, R. T. Klingbiel, D. P. Specht, P. N. Tyminski, H. Ringsdorf and D. F. O'Brien, *J. Am. Chem. Soc.*, 1984, **106**, 1627.
- 8 A. Anikin, V. Chupin, M. Anikin and G. Serebrennikova, *Makromol. Chem.*, 1993, **194**, 2663.
- 9 A. Akimoto, K. Dorn, L. Gros, H. Ringsdorf and H. Schupp, *Angew. Chem., Int. Ed. Engl.*, 1981, **20**, 90.
- 10 Y. Matsushita, E. Hasegawa and K. Eshima, *Makromol. Chem., Rapid Commun.*, 1987, **8**, 1.
- 11 S. L. Regen, A. Singh, G. Oehme and M. Singh, *J. Am. Chem. Soc.*, 1982, **104**, 791.
- 12 S. L. Regen, K. Yamaguchi, N. K. P. Samuel and M. Singh, *J. Am. Chem. Soc.*, 1983, **107**, 42.
- 13 N. K. P. Samuel, M. Singh, K. Yamaguchi and S. L. Regen, *J. Am. Chem. Soc.*, 1985, **107**, 42.
- 14 H. Ohno, Y. Ogata and E. Tsuchida, *J. Polym. Sci., Polym. Chem. Ed.*, 1986, **24**, 2959.
- 15 H. Ohno, S. Takeoka and E. Tsuchida, *Bull. Chem. Soc. Jpn.*, 1987, **60**, 2945.
- 16 H. Ohno, Y. Ogata and E. Tsuchida, *Macromolecules*, 1987, **20**, 929.
- 17 E. Tsuchida, E. Hasegawa, N. Kimura, M. Hatashita and C. Makino, *Macromolecules*, 1992, **25**, 207.
- 18 K. Akama, K. Awai, S. Tokuyama, T. Satoh, F. Hosoi and H. Omichi, *Radiat. Phys. Chem.*, 1995, **46**, 257.
- 19 K. Morizawa, K. Akama, Y. Kawakami and E. Tsuchida, *Biomater. Artif. Cells Immobil. Biotechnol.*, 1992, **20**, 641.
- 20 F. Hosoi, H. Omichi, K. Akama, K. Awai, S. Tokuyama and T. Satoh, *Nucl. Instrum. Methods Phys. Res., Sect. B*, 1995, **105**, 318.
- 21 D. Chapman, in *Form and Function of Phospholipids*, ed. G. B. Ansell, J. N. Hawthorne and R. H. C. Dawson, Elsevier Scientific, Amsterdam, 1973, p. 117.
- 22 S. Takeoka, H. Iwai, H. Ohno and E. Tsuchida, *Bull. Chem. Soc. Jpn.*, 1989, **62**, 102.
- 23 L. D. Mayer, M. J. Hope, P. R. Cullis and A. S. Janoff, *Biochim. Biophys. Acta*, 1985, **817**, 193.
- 24 K. Ogino, M. Goto and M. Abe, *J. Jpn. Oil Chem. Soc.*, 1988, **37**, 640.
- 25 T. Kagiya, M. Izu, S. Machi and K. Fukui, *Bull. Chem. Soc. Jpn.*, 1967, **40**, 1049.
- 26 T. Kagiya, M. Izu and K. Fukui, *Bull. Chem. Soc. Jpn.*, 1967, **40**, 1045.
- 27 H. Ohno, S. Takeoka, H. Iwai and E. Tsuchida, *J. Polym. Sci. Polym. Chem. Ed.*, 1987, **25**, 2737.
- 28 H. Sakai, S. Takeoka, H. Yokohama, H. Nishide and E. Tsuchida, *Polym. Adv. Technol.*, 1992, **3**, 389.
- 29 H. Ringsdorf and H. Schupp, *Am. Chem. Soc., Div. Org. Coat. Plast. Chem., Pap. Meet.*, 1980, **42**, 379.
- 30 F. Hosoi, H. Omichi, K. Akama, K. Awai, S. Endo and Y. Nakano, *Nucl. Instrum. Methods Phys. Res., Sect. B*, 1997, **131**, 329.
- 31 D. J. Hanahan, *Biochem. Prep.*, 1962, **9**, 55.